Cryogenics 65 (2015) 26–37

Contents lists available at ScienceDirect

Cryogenics

journal homepage: www.elsevier.com/locate/cryogenics

Design and performance of a fast thermal response miniature Chromium Potassium Alum (CPA) salt pill for use in a millikelvin cryocooler

J. Bartlett *, G. Hardy, I.D. Hepburn

Mullard Space Science Laboratory, Department of Space and Climate Physics, UCL, Dorking, Surrey RH5 6NT, United Kingdom

ARTICLE INFO

Article history:
Received 3 June 2014
Received in revised form 27 October 2014
Accepted 6 November 2014
Available online 18 November 2014

Keywords:
Adiabatic demagnetisation
Magnetic cooling
Millikelvin
Eddy current heating
Thermal boundary resistance

ABSTRACT

The design and performance of a fast thermal response miniature (24 mm outer diameter by 30 mm long) Chromium Potassium Alum (CPA) salt pill is described. The need for a fast thermal response has been driven by the development of a continuously operating millikelvin cryocooler (mKCC) which uses 2 T superconducting magnets that can be ramped to full field in 30 s. The consequence of magnetising and demagnetising the CPA pill in such a short time is that thermal boundary resistance and eddy current heating have a significant impact on the performance of the pill, which was investigated in detail using modelling. The complete design of a prototype CPA pill is described in this paper, including the methods used to minimise thermal boundary resistance and eddy current heating as well as the manufacturing and assembly processes. The performance of the prototype CPA pill operated from a 3.6 K bath is presented, demonstrating that a complete CPA cycle (magnetising, cooling to bath and demagnetising) can be accomplished in under 2.5 min, with magnetisation and demagnetisation taking just 30 s each. The cold finger base temperature of the prototype varies with demagnetisation speed as a consequence of eddy current heating; for a 30 s demagnetisation, a base temperature of 161 mK is obtained, whilst for a 5 min demagnetisation, a base temperature of 149 mK was measured (both from a 3.6 K and 2 T starting position). The measured hold times of the CPA pill at 200 mK, 300 mK, and 1 K are given, proving that the hold time far exceeds the recycle time and demonstrating the potential for continuous operation when two ADRs are used in a tandem configuration. The ease and speed at which the CPA pill temperature can be changed and controlled when stepping between operating temperatures in the range of 200 mK to 4 K using a servo control program is also shown, once again highlighting the excellent thermal response of the pill. All of the test results are in good agreement with the modelling used to design the CPA pill, giving good confidence in our ability to understand and estimate the effects of eddy current heating and thermal boundary resistance. To conclude, the design for the CPA pill to be used in the mKCC (which is heavily based on the design of the prototype) is presented.

1. Introduction

An Adiabatic Demagnetisation Refrigerator (ADR) consists of a salt pill (a paramagnetic material encased in an outer housing with a thermal bus for interfacing to the other parts of the ADR), a magnet and a heat switch which allows connection of the salt pill to the heat bath as shown in Fig. 1.

The operation (also known as the recycling process) of a single ADR is as follows: (1) an external magnetic field is applied to the salt pill which generates heat within the pill; (2) the heat generated during magnetisation is then removed to the heat bath via the heat switch; (3) the salt pill is isolated from the heat bath by opening the heat switch and the magnetic field is removed resulting in cooling. The ideal process (which assumes isothermal magnetisation and adiabatic demagnetisation) is shown on an entropy–temperature diagram in Fig. 2.

The base temperature of the ADR is the lowest temperature that can be achieved i.e. when the salt pill has been fully demagnetised and 0 T is reached. For useful cooling however, the salt pill is only partially demagnetised until a desired operating temperature (which must be greater than the base temperature) is reached. The remaining magnetic field is then removed at a rate such that the cooling produced from demagnetisation counteracts the heat flows into the salt pill thereby maintaining a constant operating temperature or hold temperature (T_h). The total energy Q, that can be absorbed by the pill at this temperature before zero magnetic field is reached is illustrated in Fig. 3 by the grey shaded area

* Corresponding author. Tel.: +44 1483 204206.
E-mail address: j.bartlett@ucl.ac.uk (J. Bartlett).

http://dx.doi.org/10.1016/j.cryogenics.2014.11.004
0011-2275/© 2014 The Authors. Published by Elsevier Ltd.

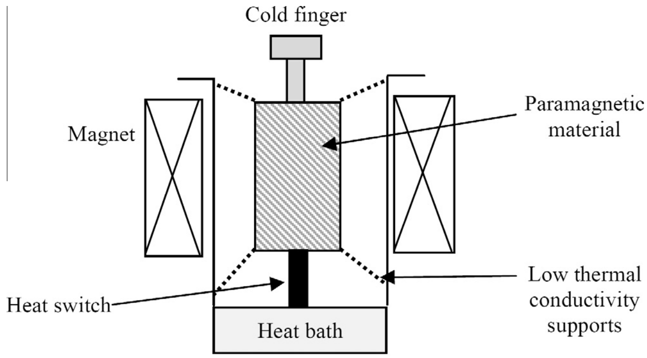

Fig. 1. Single ADR schematic.

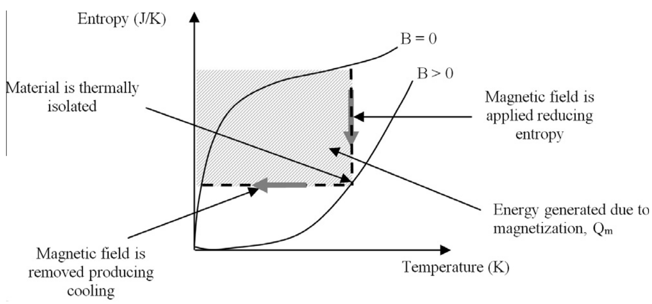

Fig. 2. Variation of entropy and temperature of a paramagnetic material during the ideal process of magnetic cooling.

and is given by $Q = nT_h(S_f - S_i)$ where n is the number of moles of material (e.g. CPA) and S_f and S_i are the final and initial entropies. The duration for which the operating temperature can be maintained and hence cooling can be provided, is called the hold time.

A double ADR (dADR), in comparison to a single ADR, utilises two (typically different) salt pills and two heat switches in a series configuration, in which one salt pill is used to precool the other to a temperature below that of the bath. The miniature millikelvin cryocooler (mKCC) being built at the Mullard Space Science Laboratory (MSSL) [1] uses Gadolinium Gallium Garnet (GGG) and Chromium Potassium Alum (CPA) as the paramagnetic materials in its two dADRs which are both linked to a single thermal interface via additional heat switches (as shown in Fig. 4). By operating the dADRs in a tandem configuration (i.e. one dADR is recycled whilst the second provides cooling), the thermal interface can be maintained at a constant temperature thereby providing continuous cooling at any user-specified temperature in the range of 100 mK to 4 K. In the mKCC, single crystal tungsten magnetoresistive heat switches are used [2]. Detailed information on the mKCC is given in Bartlett et al. [1]).

Whereas in a single shot ADR the size of the paramagnetic material (and hence the full ADR) is dependent on the energy to be absorbed over a required hold time (where typically the hold time >> recycle time), in a tandem ADR, the paramagnetic material only needs to be sized so that the hold time for a chosen cooling power exceeds the recycle time, allowing for much smaller ADRs. In addition, for a given sized tandem ADR, the maximum cooling power can be increased if the recycle time can be reduced. Therefore it is important to be able to recycle the ADR as quickly as possible to reduce the ADR size and increase its cooling power. To enable this, we have developed superconducting magnets that can be ramped from 0 to 2 T within 20–30 s and thus this set the baseline for the speed of the mKCC.

We describe below a miniature (24 mm outer diameter by 30 mm long) fast thermal response prototype CPA pill that has been built and tested as part of the mKCC development. We discuss the design process (Section 2), the manufacturing and growth procedures (Section 3) and we demonstrate the performance of the pill by presenting the experimental test results (Section 4). To conclude, in Section 5, we present the final design of the CPA pill to be used in the mKCC which is based on the prototype.

2. Prototype CPA pill design

A standard CPA pill is comprised of CPA crystals, a thermal bus which provides a thermal interface to the crystals and the other parts of the ADR, and an outer housing that hermetically seals the CPA to prevent water loss. The thermal bus is typically constructed from a high thermally conducting and low heat capacity material such as Oxygen Free High Conductivity (OFHC) copper or gold [3–5].

To achieve a fast thermal response, the design of the thermal bus is crucial in terms of the thermal boundary resistance that occurs between the thermal bus and the CPA crystals, and the eddy current heating that arises in the thermal bus due to it being subjected to a rapidly changing magnetic field. Both of these, when not minimised, result in the CPA pill having a slower thermal response, longer recycle times and shorter hold times (hence poorer performance). The effects of thermal boundary resistance and eddy current heating on the pill design were investigated and are detailed in Sections 2.1 and 2.2 respectively.

2.1. Thermal boundary resistance

In non-electrically conducting materials, such as the CPA crystals, heat is transferred by the conduction of phonons. The transfer of thermal energy by phonons across a boundary is given by Eq. (1) [6], where dQ/dt is the heat flow across the boundary, A is the contact area, T_1–T_2 the temperature difference across the boundary and β the thermal transport parameter. The value of dQ/dt is strongly dependent on temperature, therefore at low temperatures, a large temperature gradient can exist across a boundary; this is a severe problem at temperatures in the 100 mK region thereby necessitating either very low energy exchange across the boundary or large contact surface areas. Previously measured values for β are $3 \times 10^{-5}\,\mathrm{W\,cm^{-2}\,K^{-3}}$, $6.7 \times 10^{-4}\,\mathrm{W\,cm^{-2}\,K^{-3}}$ and $4 \times 10^{-4}\,\mathrm{W\,cm^{-2}\,K^{-3}}$ [7,8,3].

$$\frac{dQ}{dt} = \frac{\beta A}{3}\left(T_1^3 - T_2^3\right) \quad (1)$$

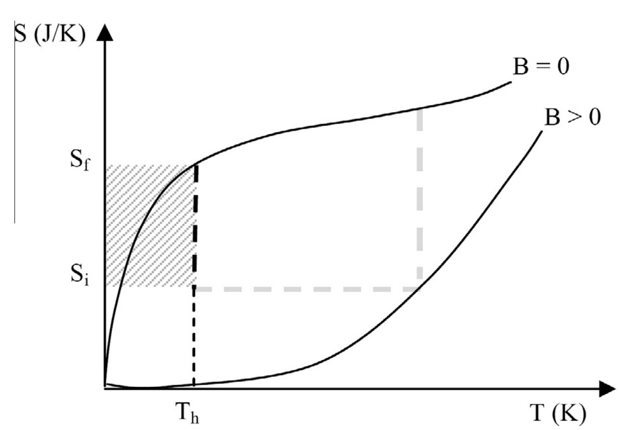

Fig. 3. Total energy that can be absorbed by a paramagnetic material at hold temperature T_h.

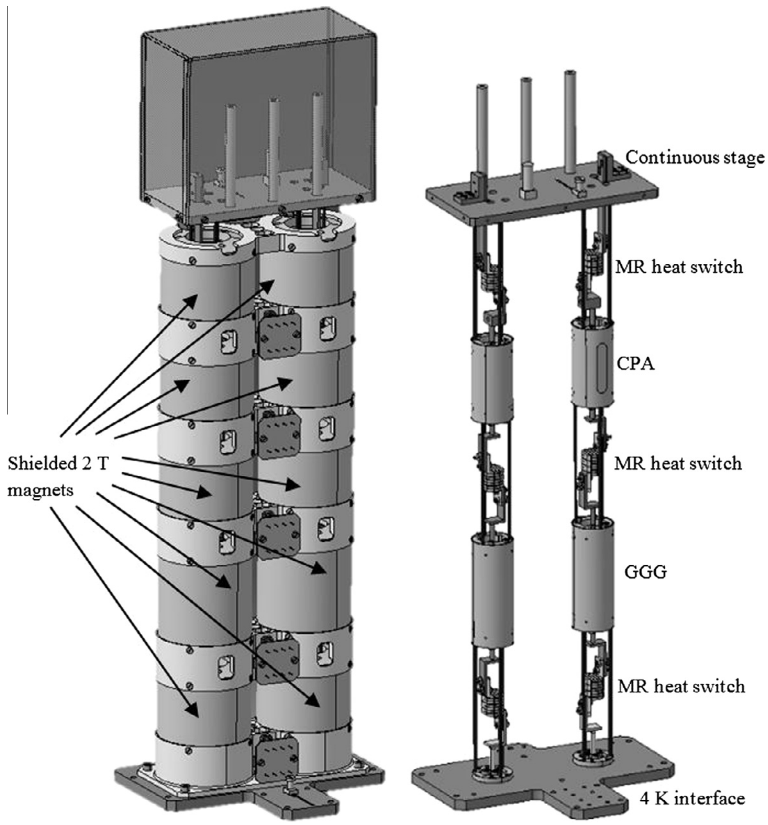

Fig. 4. The millikelvin cryocooler (mKCC). Left: the full mKCC. Right: the mKCC ADR insert.

In the CPA pill, the thermal boundary arises between the CPA crystals and the copper thermal bus. As heat flows into the CPA pill, a temperature difference is created between the CPA crystals and the thermal bus (and hence the cold stage), as governed by Eq. (1). During the hold time, a servo control program is typically used to maintain a constant temperature on the cold stage. This is achieved by the program adjusting the temperature of the CPA crystals (in relation to the cold stage temperature) through magnetisation and demagnetisation, thereby responding to, and compensating for, the heat loads on the CPA pill. Problems arise however when the heat load is sufficiently large enough that whilst trying to achieve the necessary temperature difference to maintain the stage temperature, zero magnetic field is reached, thereby ending operation at that temperature. Larger heat loads can be absorbed by the pill by minimising the thermal boundary resistance and therefore having the correct thermal boundary contact area between the thermal bus and the CPA crystals is crucial.

The CPA pill design requirements of the mKCC [1] were to 1) operate with fast ramping (0 to 2 T in 20–30 s) superconducting magnets and 2) continuously provide 1 μW of cooling power at 100 mK. An applied heat load of 1 μW was chosen to match previous ADR cooling powers based on detector requirements [3]. Based on the minimum magnet ramp rate of 20–30 s, the target recycle time for each dADR chain in the mKCC was set to 10 min. To achieve continuous cooling and to allow sufficient margin in the design, the target hold time for each CPA pill at 100 mK with a 1 μW applied heat load (in addition to the system parasitic heat loads) was set to 60 min; if the margin is not needed then greater cooling powers will be possible because the hold time can be reduced so that it just exceeds the recycle time.

A dynamic mathematical thermal model, which calculates all heat flows, entropies and temperatures within the mKCC over the full operational cycle, has been used to investigate the effect on the CPA pill hold time due to varying the contact area between the copper thermal bus and the CPA crystals; it is a trade-off between the gain in performance (hold time) achieved due to a greater contact area and hence smaller thermal boundary and the loss in performance due to the loss in volume (and hence mass) of CPA crystals. The hold times have been calculated for the CPA when operating as part of the mKCC, with the GGG stage at a temperature of 1.5–1.6 K during the hold time. For this investigation, the CPA pill size remains fixed, with an outer diameter of 24 mm and a height of 30 mm and the contact area has been varied by changing the number of 0.25 mm diameter (30 mm long) wires within the pill volume.

Fig. 5 shows how the predicted 100 mK hold time of a CPA pill operating in the mKCC, is expected to vary with contact area and applied heat load. For each applied heat load, there is a maximum (i.e. optimum) useful contact area between the CPA crystals and thermal bus, above which the hold time starts decreasing due to the reduced CPA crystal mass. There is also a minimum contact area (shown in Fig. 6) required in order to operate the mKCC so that it provides continuous cooling (i.e. the hold time of each CPA pill is greater than the recycling time of each dADR chain). This minimum represents a sharp cut-off, below which there is no continuous cooling. This is because whilst the cold CPA pill maintains the temperature of the continuous stage, the CPA pill in the other dADR chain recycles, which provides a varying heat load (with a peak during magnetisation), that has to be absorbed by the cold CPA pill. For contact areas below the minimum, the temperature difference required between the CPA crystals and the continuous stage in order to compensate for the peak heat load is too large and zero magnetic field is reached. This results in the continuous stage warming up until the heat load is reduced. At the minimum contact area, the peak heat load is just absorbed by the cold CPA pill without zero magnetic field being reached and as the heat load

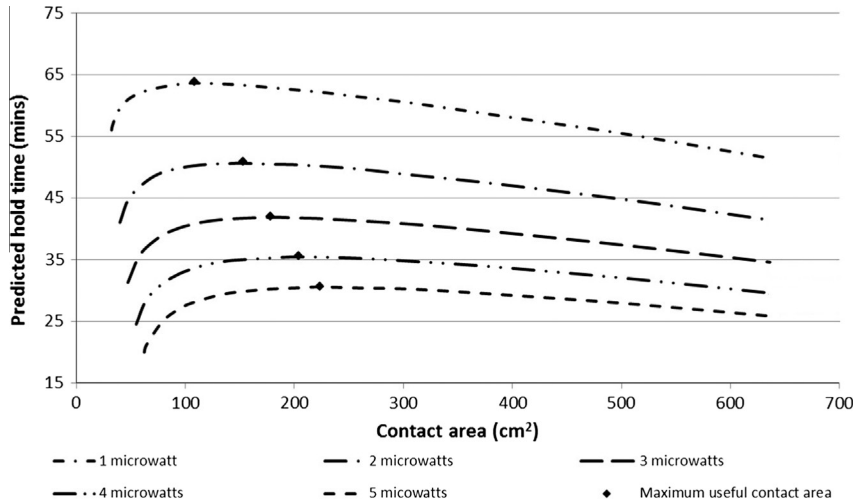

Fig. 5. Effect of contact area within the CPA pill on the predicted hold time at 100 mK for different applied heat loads.

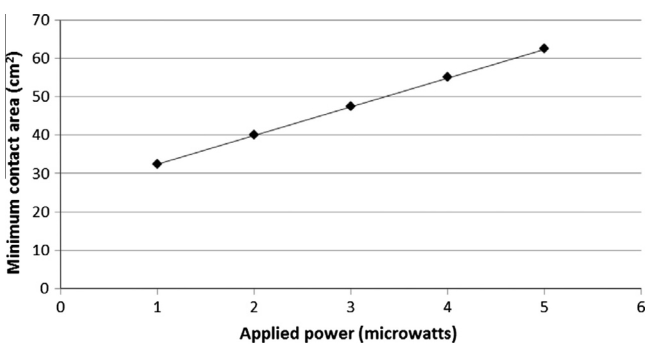

Fig. 6. Minimum contact area required in the CPA pill for operation at 100 mK for different applied heat loads.

decreases (the recycling CPA pill is demagnetised), the temperature difference decreases and continuous cooling is achieved.

Figs. 5 and 6 demonstrate the need to have the correct contact area in order to minimise the thermal boundary. For the mKCC design specification to provide 1 μW of cooling power, the minimum contact area needed to achieve continuous cooling is 32.5 cm^2 and the optimum contact area is 108 cm^2, but in comparison, for a 5 μW applied heat load at 100 mK, the minimum contact area required is 63.6 cm^2 (almost double that required for 1 μW) and the optimum contact area is 229 cm^2. It should be noted that 5 μW is the potential maximum cooling power of the mKCC if the design margin between the recycle and hold time is reduced so that the hold time only just exceeds the recycle time.

In order to achieve the design requirement of a 60 min hold time with a 1 μW applied heat load, the contact area needs to be at least 48.35 cm^2. Based on the thermal boundary resistance analysis, the target range for the contact area for the mKCC CPA pill design was set to between 63.6 cm^2 to 108 cm^2 i.e. between the minimum area required to operate with a 5 μW applied heat load (the maximum potential cooling power of the mKCC) and the optimum area for operation with a 1 μW applied heat load.

2.2. Eddy current heating

Eddy currents are electrical currents induced in a conductor when it is exposed to a changing magnetic field due to Faraday's law of induction. They oppose the original magnetic field that caused them (Lenz's Law) and generate heat in the conductor; heating is proportional to the square of the rate of change of the magnetic field and the inverse of the materials electrical resistivity, therefore the faster the magnetic field is changed the more heat is generated. Low electrical resistivity metals (such as OFHC copper or gold) are required for a thermal bus in order to ensure high thermal conductivity and hence changing to a higher electrical resistivity material is not an option for reducing eddy current heating.

The CPA pill uses a copper thermal bus and will be subjected to very rapidly changing magnetic fields of zero to two T in as little as 20 s, therefore it is important that eddy current heating is minimised as the CPA pill will have to absorb the heat generated by the eddy currents; higher heat loads will compromise the minimum achievable temperature and lead to shorter hold times.

The aim of the eddy current analysis of the thermal bus (shown in Fig. 7) is to minimise the total eddy current heating, with the analysis broken down into two Sections: (1) the end plates to which the interface straps are attached; (2) the main part of the thermal bus which is used to minimise thermal boundary resistance within the CPA pill.

2.2.1. End plate design

The CPA pill uses copper end plates to provide a good thermal interface to the other parts of the thermal bus (Fig. 7). The eddy

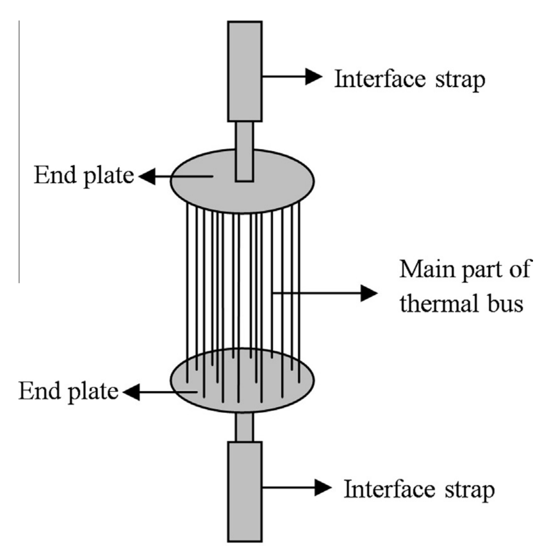

Fig. 7. CPA pill thermal bus layout.

current heating was investigated for 0 to 2 T magnet ramp times of 20, 30 and 60 s using Opera 3D, a commercially available finite element electromagnetic design software. Fig. 8 (left) shows the modelled eddy currents generated in a flat (23 mm diameter, 0.5 mm thick) copper disk with the arrows representing the magnitude of the eddy currents. For a 20 s ramp time, the eddy currents are predicted to generate 1890 μW of power, which decreases to 219 μW for a 60 s ramp time. It is well known that eddy currents are reduced by the inclusion of slits; Table 1 shows the reduction in eddy current heating as a function of the number of slits and magnet ramp time with Fig. 8 middle showing the eddy current heating in a copper disk with 8 slits. We have identified that if each segment created by the slits has additional tangential slits (as shown in Fig. 8 right) the eddy current heating is further reduced by a factor of 6 (see Table 1: 8 slits plus circular slits). Optimising the design for manufacture (8 slits plus square slits) as shown in Fig. 9 afforded a further slight reduction in the modelled eddy current heating as can be seen in Table 1.

Table 1
Eddy current heating in a flat copper disk depending on the number of radial slits and magnet ramp time.

No. of radial slits	Power generated by eddy currents (μW)		
	20 s ramp	30 s ramp	60 s ramp
0 (Fig. 8 left)	1890	824	219
1	1030	449	119
2	669	292	77
3	512	223	59
4	353	154	40
8 (Fig. 8 middle)	138	60	16
8 + circular slits (Fig. 8 right)	22.6	10	2.5
8 + square slits (Fig. 9)	19.9	8.8	2.2

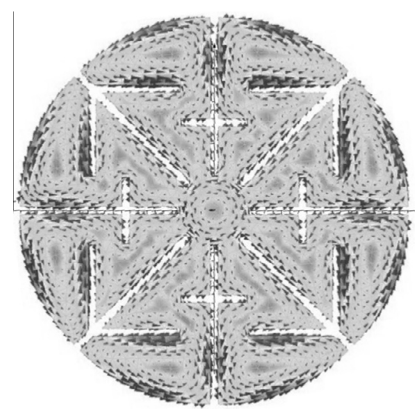

Fig. 9. Final pill end plate design with 8 radial slits and square slit design within the segments.

2.2.2. Thermal bus design

The remainder of the thermal bus incorporates the copper used to minimise the thermal boundary resistance within the pill volume. Both a slotted copper sleeve and 0.25 mm diameter copper wires within the pill were investigated. These are compared in Table 2 in terms of surface area in contact with the CPA crystals (which is important for minimising thermal boundary resistance) and the eddy current heating generated during ramping of the magnet. Fig. 10 shows the modelled eddy currents generated in the copper outer sleeve which has 23 partial vertical slits and one complete slit. The contact area provided by this copper sleeve is 18.13 cm^2, and for a 60 s magnet ramp, the modelled eddy current heating is 1.15 μW. In comparison, as shown in, Table 2 76 wires provide approximately the same contact area but the modelled eddy current heating is only 8.28×10^{-3} μW. Therefore in order to minimise eddy current heating it is much better to use wires rather than a sleeve.

Based on experience of growing CPA crystals in the laboratory, crystals of typically 1 mm diameter are easily formed and therefore the maximum pitch of the wire spacing on the end plates was set to be 1.2 mm. This spacing ensures that when grown, each CPA crystal is attached to at least one wire, maximising the heat transfer between the copper thermal bus and the CPA crystals and hence minimising the thermal boundary between the two. Using a larger pitch for the wire spacing would result in some crystals not being formed on the wires thereby creating an additional crystal to crystal boundary, reducing the efficiency of the heat transfer from the crystals to the thermal bus and hence increasing the overall thermal boundary.

By using a 1.2 mm pitch, the end plate design shown in Fig. 9 can accommodate 252 wires giving a contact area of 59.4 cm^2. This does not meet the requirement contact area range specified for the mKCC CPA pill (63.6–108 cm^2) as discussed in Section 2.1, therefore for the mKCC CPA pill, the wire pitch spacing was reduced to 1 mm to give a contact area of 87.36 cm^2 and meet the design requirement (discussed further in Section 5). Due to the initial confidence in the ability to manufacture the pill, it was decided that the 1.2 mm pitch with 252 wires, was sufficient for a prototype demonstration of a single CPA pill, operated from a 3.6 K bath; the prototype pill would not be able to reach 100 mK making the need for a larger contact area in the prototype unnecessary.

The eddy current heating contribution from 252 wires is 0.25 μW for a ramp time of 20 s, 0.11 μW for a ramp time of 30 s and 0.03 μW for a 60 s ramp time. Combining the eddy current heating contributions from the end plates and the wires, the total

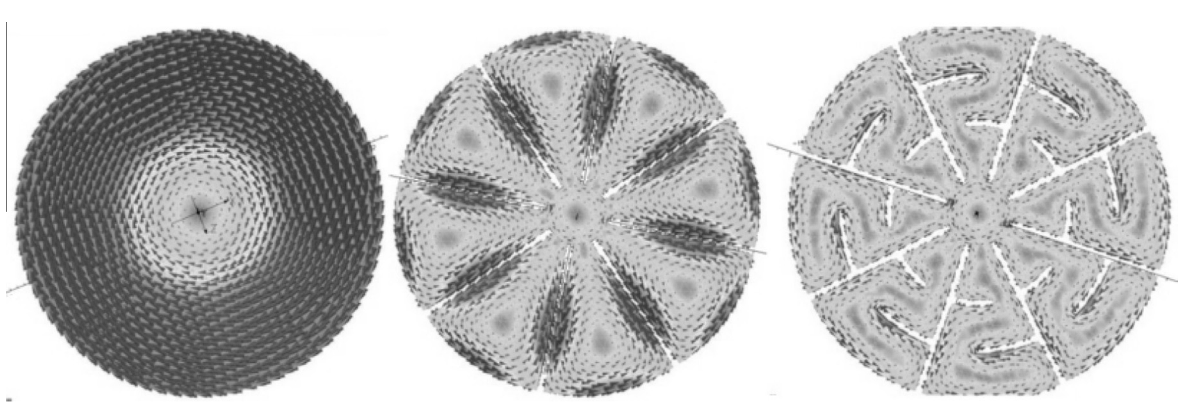

Fig. 8. Modelled eddy currents generated in copper disks with different designs: left: a flat copper disk. Middle: a flat copper disk with 8 radial slits. Right: a flat copper disk with 8 radial slits and segment slits.

Table 2
Copper outer sleeve and single wires comparison.

Component	Contact area (cm^2)	Volume of copper (cm^3)	Power generated by eddy currents (μW)		
			20 s ramp	30 s ramp	60 s ramp
Outer sleeve	18.13	0.865	10.36	4.60	1.15
Single wire	0.24	1.47×10^{-3}	9.83E−4	4.37E−4	1.09E−4
76 wires	18.24	0.112	7.47E−2	3.32E−2	8.28E−3

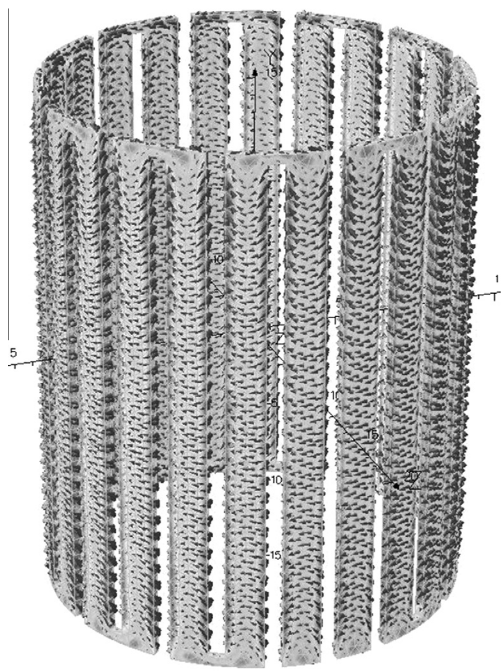

Fig. 10. Eddy currents in a copper outer sleeve with 24 slits including one full slit.

estimated eddy current heating contributions are 40.02 μW for a 20 s ramp, 17.79 μW for a 30 s ramp and 4.45 μW for a 60 s ramp time.

3. Prototype CPA pill production

There are two distinct stages in the production of the CPA pill. The first stage is the assembly of the thermal bus and the second is the growing of the CPA crystals onto the thermal bus. Both procedures are presented in detail below in Sections 3.1 and 3.2 respectively.

3.1. Thermal bus assembly procedure

Fig. 11 (left) shows the prototype CPA pill thermal bus which is comprised of: (1) two interface straps for testing; (2) two 0.5 mm thick, 23 mm diameter end plates with slits to minimise eddy current heating and 252 × 0.5 mm holes (see Fig. 11 right); 3) 252 × 0.25 mm diameter wires.

All components of the thermal bus were made from OFHC copper. The end plates were etched from 0.5 mm thick foil which gave a good finish to the end plates with no sharp edges. 0.25 mm diameter copper wires, each approximately 150 mm long were used in the assembly resulting in a total of approximately 38 m of wire being used. Each interface strap was machined from a single piece of copper.

A specially designed jig (that can be seen in Fig. 12) was used to assemble the thermal bus consisting of a base plate, two end plate mounting bracket assemblies, tie posts and mounts for the pill interface straps (which were only used once the tie posts had been removed). The end plate mounting bracket assemblies were used to hold the end plates in the correct position and at the correct separation distance of 30 mm. The tie posts were used to secure the wire ends and to keep the wires taut during the assembly process. The interface strap mounts (shown in the lower part of Fig. 12) supported the interface straps during brazing, keeping them correctly aligned in the centre of the end plates.

Each of the 252 wires were individually added to the assembly. Fig. 12 shows the assembly after approximately half of the wires have been fed through the end plates (top left) and when completed (top right).

Once the assembly was completed, the wires were vacuum brazed onto the end plates, with each wire being effectively individually brazed. The excess wire was then removed, leaving the wire ends flush with the surface of the end plates. A second brazing run was used to bond the interface straps to the end plates completing the thermal bus assembly as shown in the lower left part of Fig. 12. The entire assembly was cleaned and plated with 2–3 μm of gold to prevent oxidisation of the copper and potential erosion by the CPA. The thermal bus was assembled with the G10 outer housing using Stycast 2850 FT black ready for the crystal growing phase (bottom right of Fig. 12).

3.2. CPA pill growth procedure

The CPA crystals were grown directly onto the thermal bus within the outer housing. Saturated CPA solution was made prior to the growing of the CPA pills and stored in an airtight container ready for use; 244 grams of chromium potassium sulphate dodecahydrate were dissolved into 1 litre of ultrapure water, heated to 25 °C [9]. In order to speed up the growth of the crystals and to encourage good bonding of the crystals to the wires, CPA solution

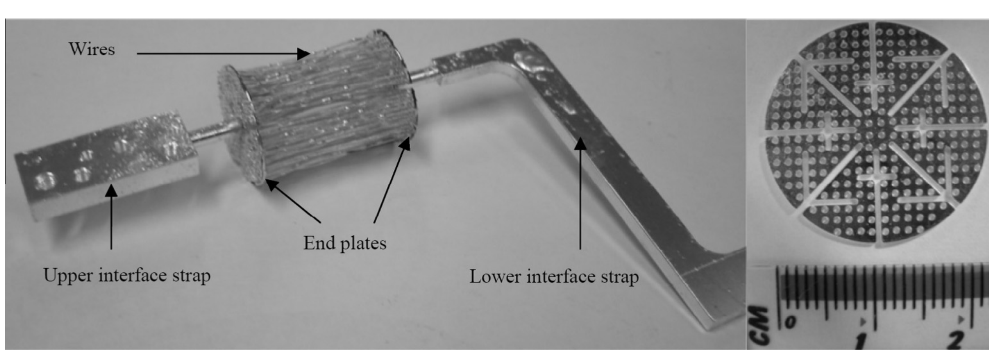

Fig. 11. Left: prototype CPA pill thermal bus. Right: end plate with 252 holes on 1.2 mm pitch.

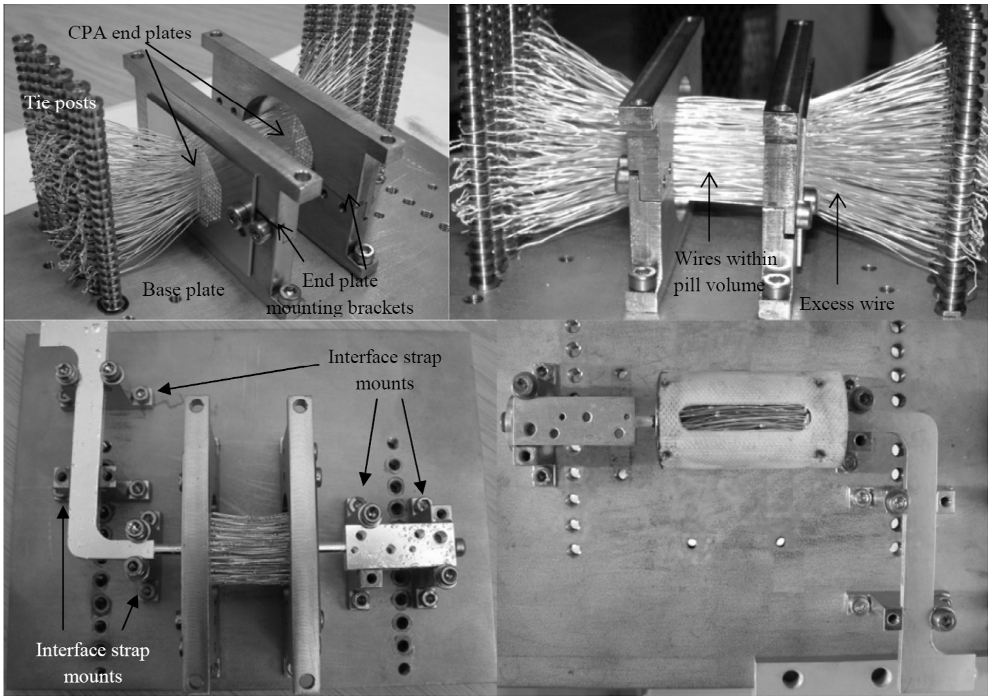

Fig. 12. Assembly of CPA thermal bus end plates and wires. Top Left: half-way through the assembly. Top right: all wires have been fed through the end plates. Bottom left: wires have been brazed to the end plates and the interface straps are attached. Bottom right: the gold plated thermal bus is assembled with the outer housing.

warmed to 30 °C was injected into the CPA pill using a needle and syringe, whilst the thermal bus was cooled to 5 °C using Peltier coolers that were GE varnished onto the interface straps (as shown in Fig. 13). The pill was grown from the base upwards in small layers, with 1–2 ml of CPA solution being added every 12–24 h; this helped prevent crystals forming on the wires at the top of the pill which could have created both air and liquid voids. As an additional measure, prior to new solution being added, the pill was rinsed using ultrapure water which ensured that any crystals that had formed higher up were dissolved and removed.

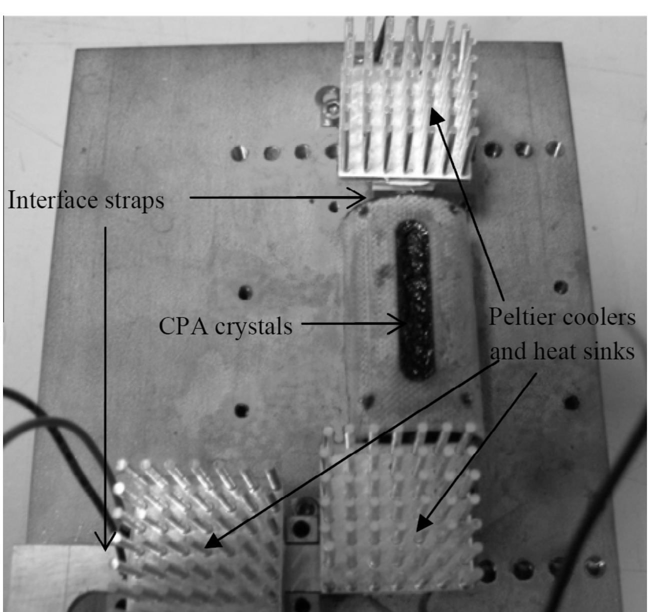

Fig. 13. Set-up for growing CPA crystals in the prototype CPA pill (the CPA pill is almost fully grown, showing the CPA crystals).

As an interesting note, it was observed that in some instances, it was difficult to grow the CPA crystals which appeared to coincide with the solution within the pill becoming thicker in consistency; in the case of any crystals being grown from this solution, their appearance was not typical of that of CPA crystals, being much larger and having very smooth surfaces. This is thought to have been linked to the temperature to which the solution was heated; whilst the target temperature was 30 °C, in some cases the hotplate would raise the solution temperature up to 35 °C (measured using a standard mercury thermometer). Stricter monitoring and control of the temperature of the solution so that it did not rise above 30 °C appeared to negate the issue.

Once grown, a layer of Stycast 2850FT black was used to seal the opening in the side of the CPA pill with the entire pill then encased in a thin layer of Stycast 1266 to prevent any water migration through the G10 whilst under vacuum.

The maximum calculated volume that can be occupied by the CPA crystals in the prototype pill is 12.03 cm^3 and the mass of CPA crystals grown within the pill is 21.85 g (43.75 mmol). Based on the known density of CPA of 1.830 g/cm^3, this gives a packing density of 99.3%

4. Prototype CPA pill testing and performance

The prototype CPA pill was tested from a 3.6 K bath (provided by a Pulse Tube Refrigerator) using one of the 2 T magnets designed and built for the mKCC. Fig. 14 shows the experimental set-up; the CPA pill is isolated from the 3.6 K base plate by a Vespel SP1/G10 suspension unit and is connected to the base plate via a mechanical heat switch. The magnet is connected to the 3.6 K baseplate via a gold plated copper support tube. A Ruthenium Oxide thermometer and a Cernox thermometer were mounted onto the CPA cold finger.

The aim of the testing was to demonstrate that the thermal response of the CPA pill is sufficient to allow magnetisation and demagnetisation in 30 s, thereby validating the design in terms of suitably minimising both thermal boundary resistance and eddy current heating as well as proving the manufacturing methods. The thermal response testing and analysis has been broken down into three sections: (i) the recycling of the CPA pill; (ii) the hold times of the pill at different operating temperatures; (iii) an operating temperature step test to determine the performance and responsiveness of the pill when stepping between different hold temperatures in the range 200 mK to 4 K. These are discussed in Sections 4.1, 4.2 and 4.3 respectively.

4.1. CPA pill recycling

The prototype CPA pill has been successfully magnetised and demagnetised in 30 s; the pill showed an immediate thermal response to the application and removal of magnetic field and upon demagnetisation the CPA cold finger was cooled from 3.6 K to 195 mK in just 30 s, demonstrating an excellent thermal link between the CPA crystals and thermal bus. Fig. 15 shows two full cycles comprising magnetisation, cooling to the bath and demagnetisation. Due to the fast thermal response, a full cycle is completed in less than 2.5 min, with 90 s of cooling being required after magnetisation (which is limited by the mechanical heat switch). It should be noted that the noise shown in Fig. 15 at the higher temperatures is due to the insensitivity at this temperature of the Ruthenium Oxide temperature sensor which typically is only used in the millikelvin region.

As discussed in Section 2.2, eddy current heating (ECH) is produced within the copper of the CPA pill when it is in a changing magnetic field. This becomes important during demagnetisation as it is an additional heat load to the CPA and therefore has an impact on the CPA pill base temperature. Table 3 gives the predicted ECH contributions for demagnetisation rates of 30, 60, 150 and 300 s, with Fig. 16 showing the measured effects of ECH in terms of the base temperature of the CPA pill cold finger; a lower base temperature is achieved with a slower demagnetisation time due to less ECH.

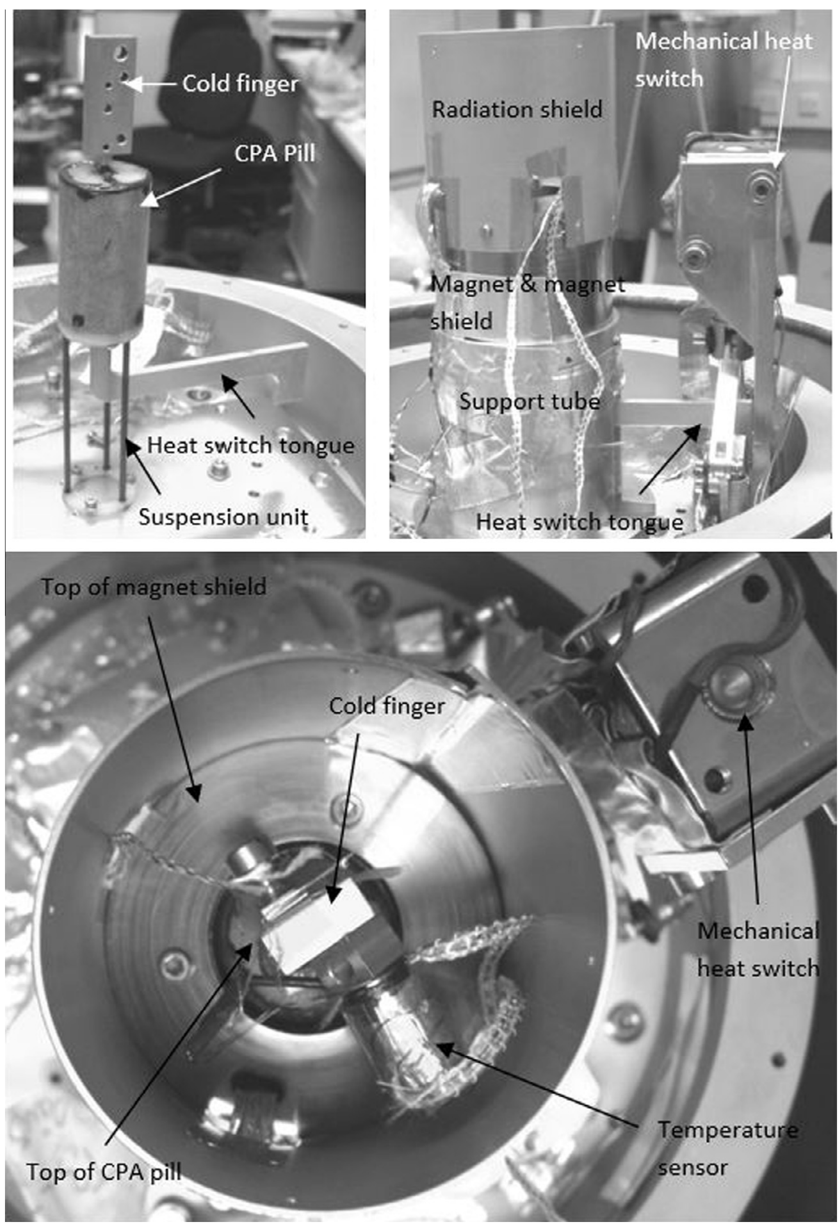

Fig. 14. Experimental set up for testing the prototype CPA pill: top left: CPA pill on its suspension unit; top right: magnet, magnet shield and radiation shield are added over the CPA pill; bottom: looking down onto the CPA and magnet assembly.

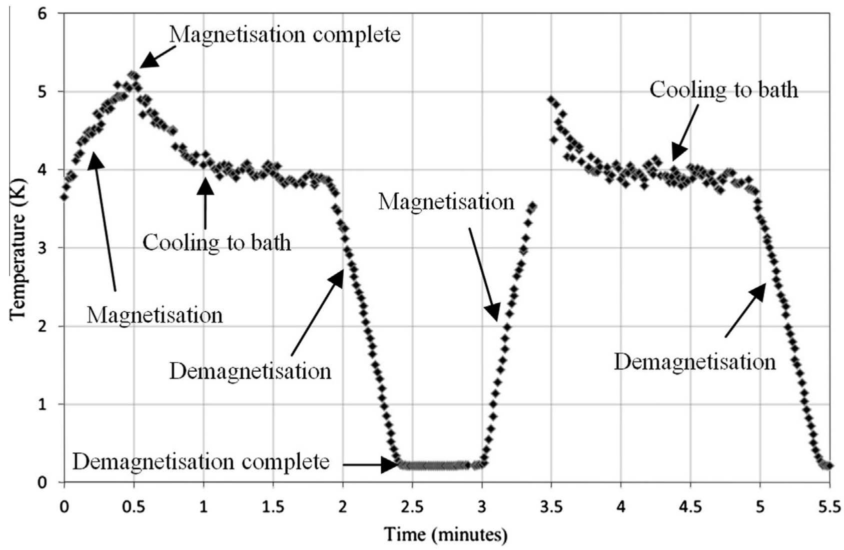

Fig. 15. Temperature of the prototype CPA pill during two magnetisation and demagnetisation cycles.

Table 3
Eddy current heating contributions for different demagnetisation times.

Demagnetisation time (s)	Eddy current heating (μW)	Total energy absorbed due to ECH (μJ)
30	17.79	533.6
60	4.45	266.8
150	0.71	106.7
300	0.18	53.3

Table 4
Thermal lag effect of ECH on the base temperature of the CPA cold finger depending on the demagnetisation rate.

Demagnetisation time (s)	Demagnetisation temperature (mK)	Time delay to achieve base temperature (s)	Base temperature (mK)	ΔT (mK)
30	195	48	161	34
60	173	42	156	17
150	161	34	152	9
300	155	33	149	6

In addition, there is a small thermal lag between zero magnetic field being reached and the base temperature on the CPA cold finger being obtained. This is a result of the ECH within the copper thermal bus generating a temperature difference between the copper and CPA crystals during demagnetisation due to the thermal boundary (which is greater for faster demagnetisation rates); when demagnetisation is complete, the ECH disappears, thereby allowing the copper to be further cooled from its demagnetisation temperature to its base temperature by the CPA crystals (see Table 4); whilst there is not significant variation in the time taken to achieve the base temperature for the different demagnetisation rates (the time delay ranges from 33 to 48 s), the amount of cooling achieved ranges from 34 mK for the 30 s demagnetisation to only 6 mK for the 300 s demagnetisation. Therein lays the trade-off depending on the system requirements in terms of demagnetisation time, cooling time and the base temperature required.

Analysis of the recycling of the prototype CPA pill validates the pill design demonstrating that a fast thermal response is achieved; the pill can successfully magnetise and demagnetise in 30 s, fully utilising the performance of the magnets. This analysis further highlights the issues associated with ECH and how important it is to minimise these effects especially as faster thermal responses are demanded.

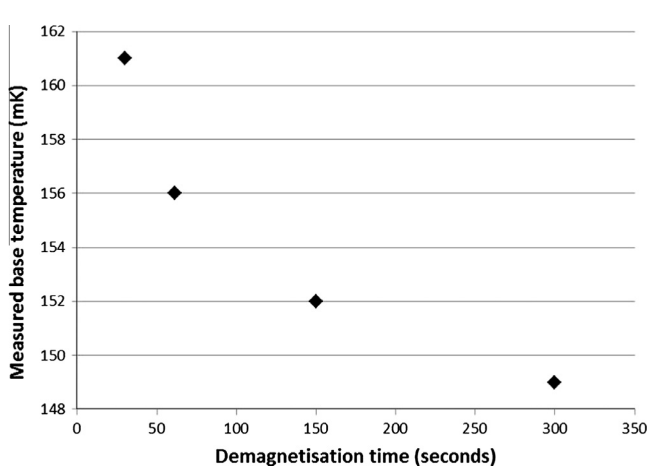

Fig. 16. CPA pill base temperature as a function of demagnetisation time.

4.2. CPA pill hold times

Measuring and analysing the hold time of the CPA pill allows the thermal boundary resistance within the pill to be assessed; the thermal boundary dictates the actual temperature of the CPA crystals in comparison to the temperature of the cold finger, which is maintained at a constant temperature by a servo control program. Fig. 17 shows the temperature profile during the recycling of the CPA pill and subsequent operation at 200 mK. During the hold time, the servo control program maintained the CPA pill temperature to within a millikelvin. It is expected that microkelvin stability can be achieved with fast read-out thermometry (which was not available at the time of testing but which will be used for the mKCC), as this would allow for temperature control on much faster (millisecond) timescales than the current (approximately 1 s) thermometry readout used.

The mathematical thermal model used to design the mKCC has been modified to simulate the prototype CPA pill test set up; the model is a 0.1 s time step dynamic model and incorporates all

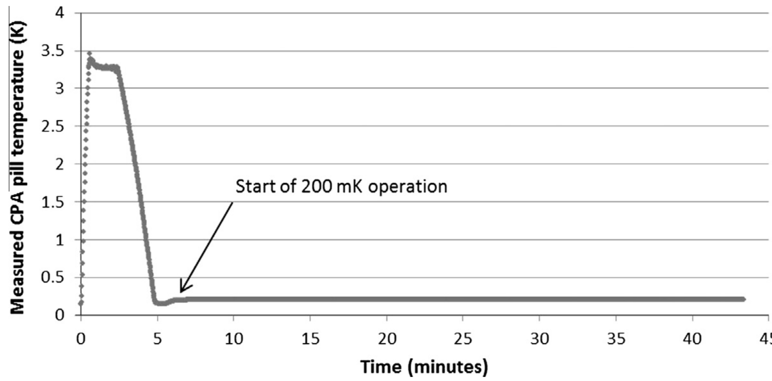

Fig. 17. Measured CPA temperature during recycling and 200 mK operation.

Table 5
Comparison of the measured and predicted hold times for the prototype CPA pill.

Operating temperature (CPA cold finger temperature) (mK)	Predicted CPA crystal temperature (mK)	Measured hold time (min)	Modelled hold time (min)
200	197.7	36.25	36.22
300	299.0	106.6	105.9
1000	999.9	574.2	570.6

material thermal conductivities and heat capacities (based on published data). It calculates the parasitic heat loads within the system along with the effects on the CPA pill entropy and temperature, throughout both the recycle and hold times. The model also takes into account the thermal boundary resistance within the CPA pill and the eddy current heating generated during magnetisation and demagnetisation; the predicted power generated by eddy current heating (as given in Table 3), is included into the model and its predicted effect on the pill entropy and temperature is calculated in the same way as for the parasitic heat loads, which for during demagnetisation, is via a process referred to as 'the step method' [10]. Using this model, with only the thermal transport parameter β set as a variable, the hold times of the CPA pill cold finger at 200, 300 and 1000 mK were predicted and compared to those measured (see Table 5). As can be seen in the table, the modelled values, which are all calculated using a value of β of 4×10^{-4} W cm^{-2} K^{-3}, are in good agreement with the measured values. This demonstrates that we have a good understanding of the thermal boundary within the CPA pill and that the analysis conducted to design the pill is a good estimate.

The hold times were measured with no applied heat load (the parasitic heat load is 2.35 μW), but there is a significant margin between the 2.5 min recycle time and the 200 mK hold time of 36.25 min; to achieve continuous cooling, the hold time only needs to just exceed the recycle time, therefore based on modelling, this CPA pill could operate at 200 mK with an applied heat load of 14 μW, which would reduce the hold time to 3 min.

4.3. Operating temperature step test

An operating temperature step test has been conducted to demonstrate the practical usability of the fast thermal response CPA pill (and hence the mKCC). During the step test, the CPA cold finger temperature is held at, and stepped to, a range of temperatures between 0.2 and 4 K as shown in Fig. 18. Each temperature is maintained for 1–2 min before the next operating temperature is selected. Once selected, the new temperature is reached within 20–30 s which is thought to be limited by the servo response time and not the thermal response of the CPA pill because an immediate thermal response is seen during magnetisation and demagnetisation (Fig. 15) when the servo program is not in control of the pill temperature; it is anticipated that the servo response time will be reduced once combined with the fast read-out thermometry.

As can be seen in Fig. 18, the CPA pill can be operated at any temperature between 100 mK and 4 K with minimal delay when transferring between operating temperatures, thereby meeting the mKCC design requirement.

5. CPA pill design for the mKCC

The success of the prototype CPA pill in terms of its fast thermal response and manufacturing methods has proven the design basis of the CPA pill for the mKCC. However, based on the thermal

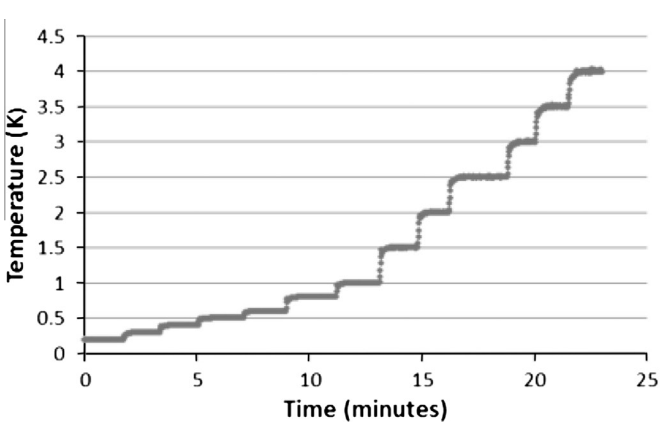

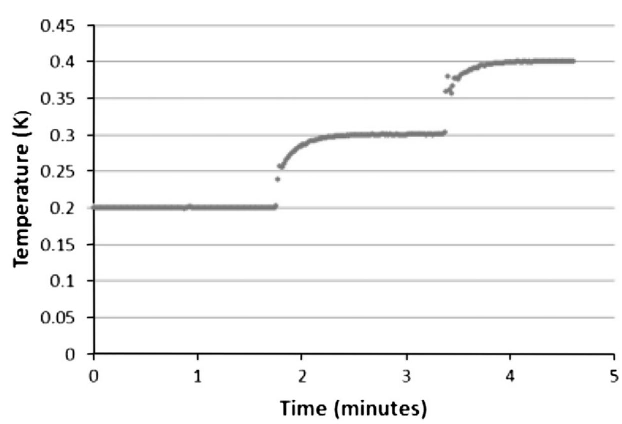

Fig. 18. Demonstrating the practical use of the fast thermal response of the CPA pill; left: the CPA pill is held at, and stepped to, temperatures between 200 mK and 4 K using a servo control program; right: a zoomed in view of the 200, 300 and 400 mK steps, highlighting the ease and speed at which the new operating temperature is reached.

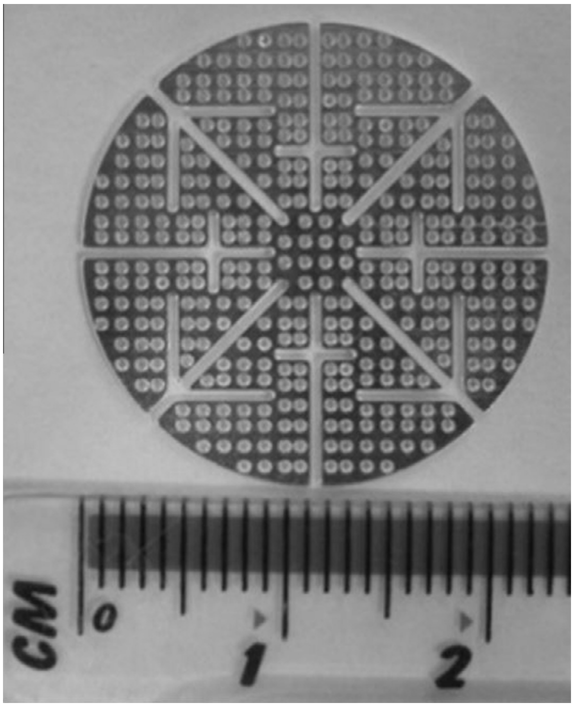

Fig. 19. mKCC CPA pill end plate with 364 holes on a 1 mm pitch.

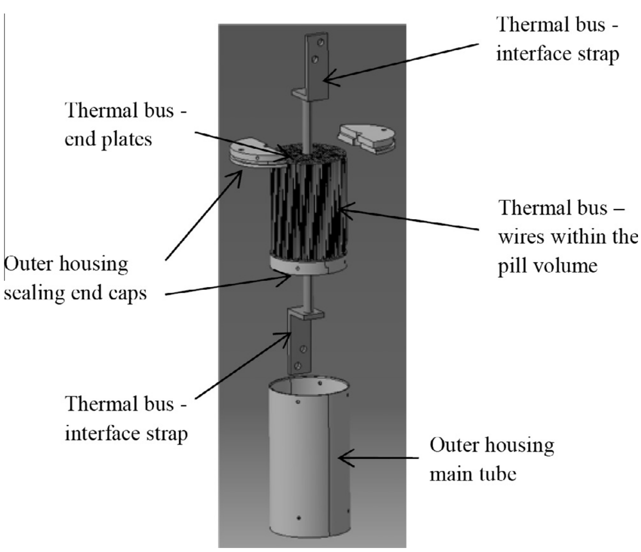

Fig. 20. Exploded view of the mKCC CPA pill.

boundary analysis in Section 2.1, the contact area between the copper thermal bus and the CPA crystals in the prototype CPA pill is not sufficient to allow 5 μW of cooling power at 100 mK which is the potential maximum cooling power of the mKCC. Therefore, in order to meet the design requirements for the mKCC CPA pill, the contact area has been increased by reducing the wire spacing pitch from 1.2 mm to 1.0 mm on the pill end plates (see Fig. 19); a 1 mm pitch allows 364 wires to be housed within the pill volume (increased from 252) which provides a contact area of 87.36 cm^2 (compared to 59.4 cm^2) thereby exceeding the 5 μW minimum contact area of 63.6 cm^2.

The additional 112 wires has marginally increased the ECH contribution due to the wires from 0.11 μW to 0.16 μW for a 30 s ramp rate, which is insignificant compared to the 17.68 μW contribution from the two end plates; the total ECH contribution for the mKCC pill is therefore 17.84 μW.

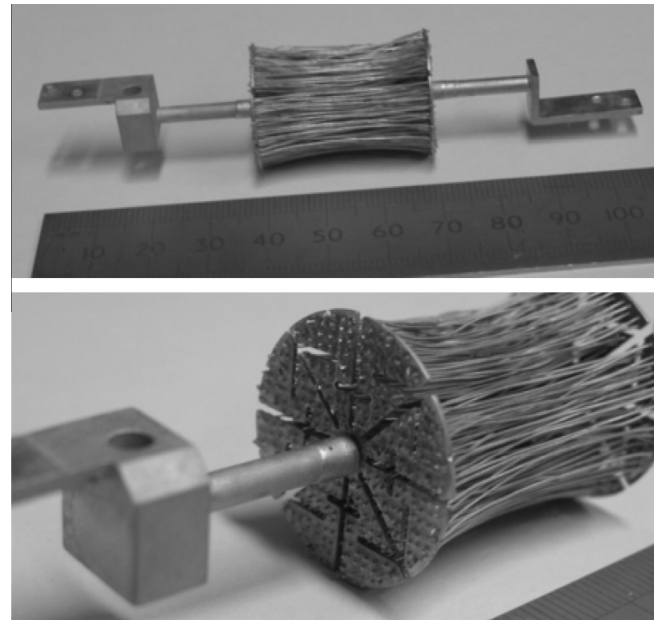

Fig. 21. 364 wire CPA thermal bus assembly for use in the mKCC. Top: side view of assembly. Bottom: end view showing the end plate design and the wire brazing.

The interface straps for the prototype CPA pill were designed specifically for the prototype test set up in order to provide a mechanical heat switch interface and a usable cold finger. For the mKCC pill, the interface straps have been modified so that the CPA pill fits with the mKCC and can interface with single crystal tungsten magnetoresistive heat switches. With the exception of an increase in the number of wires within the CPA pill volume and different interface straps, the CPA pill for the mKCC is unchanged from that of the prototype CPA pill and is shown in an exploded view in Fig. 20.

The thermal bus for the mKCC has been built and is shown in Fig. 21. The manufacturing processes used were the same as for the prototype CPA pill.

The mKCC CPA pill has been successfully grown and was tested in the summer of 2014 after the initial submission of this paper. The test set up was similar to that of the prototype CPA pill but a magnetoresistive tungsten heat switch was used instead of a mechanical one. The results will be the subject of a future publication.

6. Conclusions

A fast thermal response prototype CPA pill has been designed, built and tested, proving that it can respond to a 30 s 0 to 2 T ramp in magnetic field. As part of the design process, the effects of thermal boundary resistance and eddy current heating were investigated and methods of minimising these were incorporated into the design; the thermal boundary resistance was minimised by having a sufficient contact area between the copper thermal bus and the CPA crystals and the eddy current heating was minimised by incorporating slits into the CPA pill end plate design.

A prototype CPA pill was built which has 252 wires (which provide a contact area of 59.4 cm^2) and contains 21.85 g (43.75 mmol) of CPA. It was tested from a 3.6 K bath provided by a pulse tube refrigerator and demonstrated a fast thermal response and excellent thermal link between the copper thermal bus and CPA crystals when subjected to recycling, hold time and operating temperature step tests; the pill responded immediately to the application and removal of magnetic field with both magnetisation and demagnetisation each being accomplished in 30 s, fully utilising the performance of the superconducting magnets for the mKCC. The complete cycle (magnetisation, cooling to bath and demagnetisation) was measured to be under 2.5 min, whilst the hold time at 200 mK was measured to be 36.25 min (with no applied heat load) demonstrating the potential for continuous cooling when using two ADRs in a tandem configuration. The base temperature of the pill was measured to be 161 mK for a 30 s demagnetisation, decreasing to 149 mK for a 5 min demagnetisation due to the difference in the eddy current heating contributions. The operating temperature step tests, during which the CPA pill cold finger was held at and stepped to a range of temperatures between 0.2–4 K, further demonstrated the fast thermal response of the pill; a new operating temperature was reached within 20–30 s although this is likely limited by the servo response time.

Based on the successful performance of the prototype CPA pill, the actual CPA pill for the mKCC has been designed and built with the only differences being an increase in the number of wires (364 compared to 252) to allow for higher cooling powers and the design of the interface straps. This was successfully tested in summer 2014 and the results will be presented in a future publication.

Acknowledgements

The work presented here has been funded by the following Engineering and Physical Sciences Research Council (EPSRC) grant EP/H04888X/1. The authors would like to thank both reviewers for their helpful comments.

References

[1] Bartlett J, Hardy G, Hepburn ID, Milward S, Coker P, Theobald C. Millikelvin cryocooler for space and ground based detector systems. In: Proc SPIE 8452, millimeter, submillimeter, and far infrared detectors and instrumentation for astronomy VI; 2012: 84521O. http://dx.doi.org/10.1117/12.926250.

[2] Bartlett J, Hardy G, Hepburn ID, Ray R, Weatherstone S. Thermal characterization of a tungsten magnetoresistive heat switch. Cryogenics 2010;50(9):647–52. http://dx.doi.org/10.1016/j.cryogenics.2010.02.027.

[3] Bartlett J, Hardy G, Hepburn ID, Brockley-Blatt C, Coker P, Crofts E, et al. Improved performance of an engineering model cryogen free double adiabatic demagnetization refrigerator. Cryogenics 2010;50(9):582–90. http://dx.doi.org/10.1016/j.cryogenics.2010.02.024.

[4] Luchier N, Duval JM, Duband L, Camus P, Donnier-Valentin G, Linder M. 50 mK cooling solution with an ADR precooled by a sorption cooler. Cryogenics 2010;50(9):591–6. http://dx.doi.org/10.1016/j.cryogenics.2010.02.022.

[5] Shirron P, McCammon D. Salt pill design and fabrication for adiabatic demagnetization refrigerators. Cryogenics 2014;62:163–71. http://dx.doi.org/10.1016/j.cryogenics.2014.03.022.

[6] Ambler E, Hudson RP. Magnetic cooling. Rep Prog Phys 1955;18(1):251–303. http://dx.doi.org/10.1088/0034-4885/18/1/307.

[7] Mendoza E. Les Phénomènes Cryomagnétiques. Langevin-Perrin Colloquim, Collège de France; 1948. p. 53.

[8] Goodman BB. The thermal conductivity of superconducting tin below 1 K. Proc Phys Soc A 1953;66(3):217–27. http://dx.doi.org/10.1088/0370-1298/66/3/303.

[9] Hagmann C, Benford DJ, Richards PL. Paramagnetic salt pill design for magnetic refrigerators used in space applications. Cryogenics 1994;34(3):213–9. http://dx.doi.org/10.1016/0011-2275(94)90171-6.

[10] Bartlett J. Design of a 50 mK continuous adiabatic demagnetisation refrigerator for future space missions. PhD thesis. UCL, University of London; October 2008.